Modified Material Properties in Curved Panels Through Lamina Emergent Torsional Joints*

Trent Zimmerman¹, Jared Butler¹, Dallin Frandsen¹, Dakota Burrow¹, David Fullwood¹, Spencer Magleby¹, and Larry Howell¹

Abstract—Compliant joints have a number of advantages that make them suitable for highly constrained design problems. While much work has been done on the design of compliant joints manufactured from planar sheet materials, this work focuses on the design of cylindrically-curved joints. A method for using lamina emergent torsional (LET) joints to increase energy storage efficiency in curved sheet materials is presented. A numerical model is provided for predicting the stiffness and maximum applied moment of a curved LET joint. Predicted curved LET joint stiffnesses and maximum moments are utilized to create shape factors that produce an effective modulus of elasticity and an effective modulus of resilience. For a given case, the effective modulus of elasticity is shown to decrease by about three orders of magnitude while the effective resilience decreases by approximately one order of magnitude. Designers can use this information to tailor materials to fit design requirements or to select alternative materials that were previously unsuited for an application.

I. INTRODUCTION

Compliant joints are capable of solving highly constrained design problems due to their potential for monolithic and compact design, low mass, scalability, and suitability for harsh environments. They serve as a base component of compliant mechanism design and allow designers to create mechanisms with complex movements that exhibit these properties, making them suitable for highly constrained applications [1] such as for space [2], minimally invasive surgery [3], or microelectro mechanical systems [4]. A particular benefit of compliant joints is their capacity for energy storage. A compliant joint can be considered a traditional pin joint with an attached torsional spring [5]. A mechanism that incorporates compliant joints will be influenced by the strain energy in this spring. By identifying the maximum amount of energy that can be safely stored within the joint without plastic deformation, mechanisms can be designed to use the spring behavior of the joint to perform desired tasks, such as aid in actuation [6] or provide multistable behavior [7].

One method of creating compliant joints with energy storage capabilities is through the Lamina Emergent Torsional (LET) joint, a combination of local bending and torsional members that together produce a global hinge motion [8]. These joints can be used to create

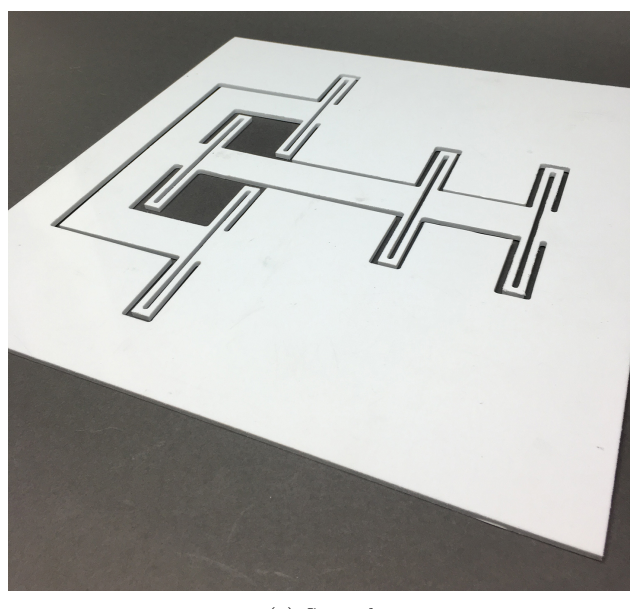
mechanisms that deploy from a surface, such as the four-bar mechanism shown in Figure 1. While traditional LET joints are formed from planar sheet material, designers would benefit from an expansion to include LET joints fabricated from a singly curved sheet, as shown in Figure 2. A curved LET joint would allow for energy storage within joints of mechanisms created out of pre-existing curved members, such as shafts, rocket bodies, needles, or wheels. Energy-storing devices developed from these surfaces could enable new or multifunctional capabilities, such as shafts with contained self-retracting deployable fins, needles with bistable anchoring devices, or impactabsorbing mechanisms on the surface of vehicles.

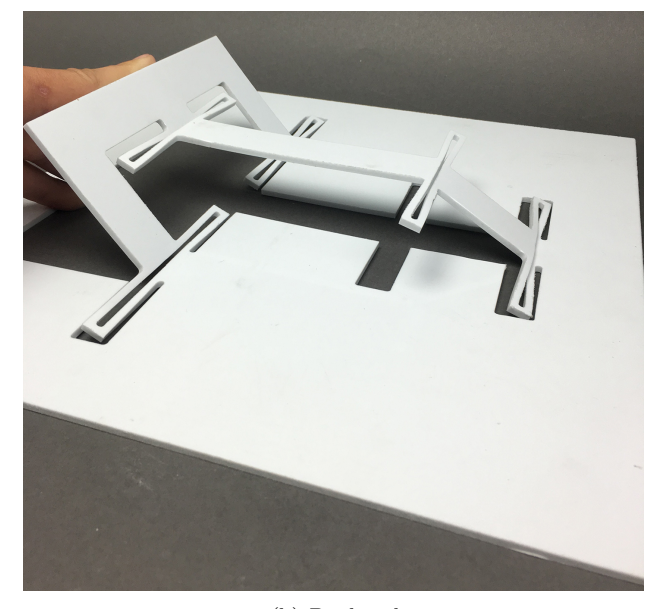
The bending and torsional members that comprise a LET joint are created by removing material from a sheet which in turn significantly reduces stiffness and influences the amount of strain energy and where strain occurs. Because this behavior is largely influenced by the geometry of these compliant segments, material selection shape factors provide an effective method of comparing LET joint energy storage properties with changes in joint stiffness. Energy stored per unit volume before yield, known as the material's modulus of resilience, allows for design with direct consideration of strain energy limits in the material. By altering the geometry of the substrate material, a "new" material can be created through the application of shape factors [9]. This new material can be considered geometrically identical to the original substrate but with adjusted (effective) material properties due to the changed shape. With these effective material properties, designers could make rapid comparisons between altered materials for design applications where energy storage and flexibility are desirable.

This paper proposes a method to derive an effective modulus of resilience and effective modulus of elasticity in curved sheet materials by developing multiple shape factors relating the stiffness and maximum moments of a singly curved LET joint to those of the uncut substrate. These shape factors will be derived by first defining the fundamental design of curved LET joints aligned longitudinally on a cylinder. Analytical and numerical models will be provided along with verification. Modification of material properties will be demonstrated on an Ashby plot [9] by applying the shape factors to compare changes in modulus of resilience against changes in modulus of elasticity for various materials.

^{*}This work was supported by the U.S. National Science Foundation.

¹Authors are with the Department of Mechanical Engineering, Brigham Young University, Provo, UT, USA trentzim@gmail.com





(a) Stowed. (b) Deployed.

Fig. 1. A four-bar Lamina Emergent Mechanism (LEM) fabricated with planar LET joints.

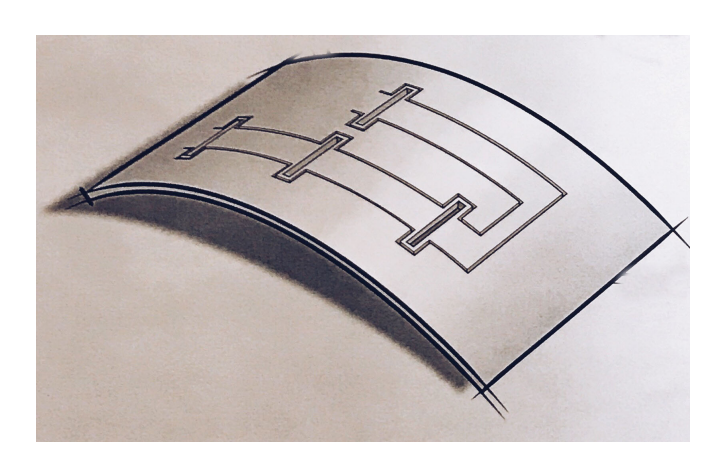


Fig. 2. A mechanism created from a cylindrically-curved sheet with incorporated curved LET joints.

II. BACKGROUND

The curved LET joint model presented in this paper is enabled through design methods and results obtained in previous investigations on compliant mechanisms, lamina emergent mechanisms, and lamina emergent torsional joints. A summary of relevant background information in these areas is discussed in this section.

A. Compliant Mechanisms

Traditional mechanisms transfer motion, force, or energy from an input to an output through rigid links and joints. Compliant mechanisms, conversely, achieve mechanism function from the deflection of flexible members [5]. Compliant mechanisms continue to demonstrate their potential for monolithic design [10], high-precision movement [11], scalability, impact-resistant design [12],

low-cost production [13], reliable performance in harsh environments [14], and energy storage [15]. The highly nonlinear behavior of compliant mechanisms can make design challenging, but the development of methods to analyze this nonlinear behavior [5], [16], [17], [18] has enabled optimization methods to predict their behavior [19], [20], [21], [22], [23]. These tools have facilitated the design of compliant mechanisms and opened the doors to a variety of new applications. This work will utilize the pseudo-rigid body model [5] to enable the analysis of curved LET joint stiffness to predict joint behavior.

B. Lamina Emergent Mechanisms

Lamina Emergent Mechanisms (LEMs) are mechanisms fabricated from planar, thin sheet materials that deploy out of plane to achieve their function. They are a subset of ortho-planar mechanisms and are compliant mechanisms [24] which makes them useful in a number of applications not suitable for traditional mechanisms. These mechanisms possess many of the same benefits as LET joints which enable the design of mechanisms such as microelectro-mechanical systems [25] and disposable devices [26].

C. Lamina Emergent Torsional Joint

LET joints are compliant joints made from a planar layer of material which rotate from a plane [8]. LET joints provide rotation by transferring the bending motion between two panels to the twisting of torsional bars which lie parallel to the joint axis (see Figure 3). They are capable of large deflections and energy storage which make them practical in many micro and macro applications.

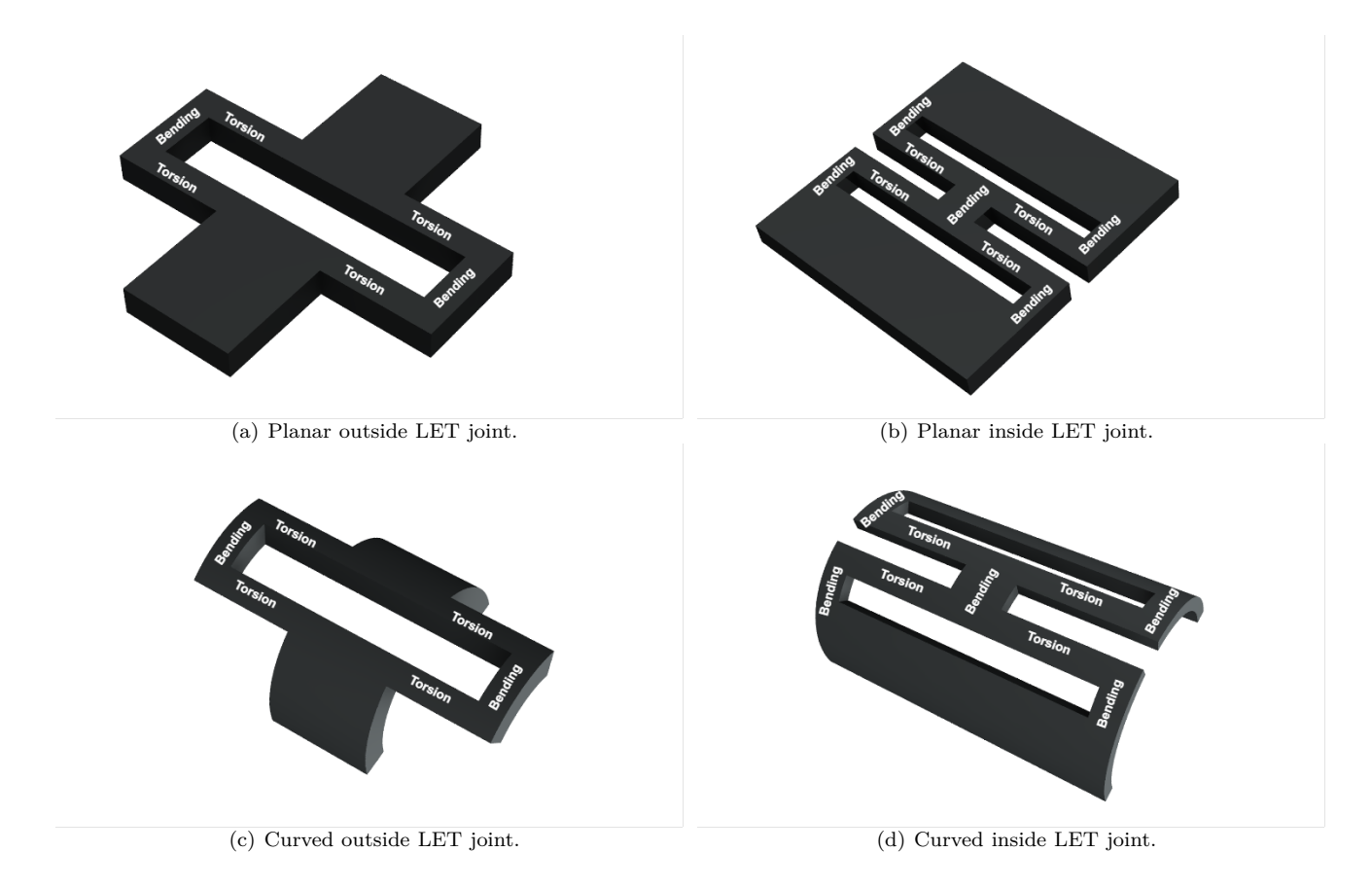


Fig. 3. The outside (a) and inside (b) LET joints. The segments placed in torsion and bending when the joint is rotated are labeled.

There are several types of LET joints which have been designed to meet specific desired motions or constraints [27], [28], [29], [30]. The outside and inside LET joints are commonly used in LEM applications [31] and are shown in Figure 3(a) and 3(b). These two configurations will be studied for curved LET joints. Because planar LET joints maintain many characteristics similar to curved LET joints, extending principles of planar LET design to curved surfaces represents the next step in advancing LET joint capabilities.

III. METHODS

This section describes a method to create "new" materials by applying LET joints to curved panels. Section III-A identifies the stiffness and resulting moment and deflection characteristics of a curved LET joint. Section III-B utilizes the identified joint stiffness to create an effective modulus of elasticity and effective modulus of resilience for curved LET joints. Section III-C describes performance indices as a method of using the derived effective modulus of elasticity and modulus of resilience to aid in rapid comparison of materials for design applications.

A. Joint Mechanics

Both curved and planar LET joints incorporate bending and torsional segments, which can be treated as

springs in parallel and series. Though the stiffness of the individual segments of the curved LET joint need to be accommodated for curvature, using a structure similar to that of existing planar LET methods [8] will permit the equivalent stiffness of a curved LET joint to be predicted. The curved LET can be modeled as a revolute hinge coupled with a torsional spring. The moment-deflection behavior of the joint rotated about its longitudinal (hinge) axis is then expressed by

$$M = k_{eq}\alpha \tag{1}$$

where k_{eq} is the equivalent stiffness per unit length of all of the torsional and bending segments of the joint and α is the deflection angle of the joint. If all of the torsional segments are equal in stiffness, k_{eq} can be found for the outside LET joint as

$$k_{eq} = \frac{2k_t k_b}{k_t + 2k_b} \tag{2}$$

and for the inside LET joint as

$$k_{eq} = \frac{k_t k_b}{5k_t + 4k_b} \tag{3}$$

where k_t and k_b are the stiffnesses of a torsional segment and a bending segment, respectively.

The differences between the planar and curved LET can be seen in the differing geometries of the bending and torsion members shown in Figure 3. The bending segments of the curved LET joint can be modeled as initially curved beams with rectangular cross sections. They are, however, assumed to be short enough to be approximated as small-length flexural pivots, which permits application of the pseudo-rigid body model [5] to determine the bending stiffness of the bending segments as

$$k_b = \frac{EI_b}{L_b} \tag{4}$$

where E is the Young's modulus of the material, I_b is the second moment of area of the bending members, and L_b is the arc length of the small-length flexural pivot measured along the centroidal axis.

The cross section of the torsional segments is an annular sector as shown in Figure 4. The torsional stiffness of a beam with an annular cross section can be found numerically through the summation [32]

$$k_{t} = \frac{4G}{L_{t}} \sum_{m=1}^{\infty} F_{m} \frac{\sin \gamma_{m} \theta_{0}}{\gamma_{m}} \left[\frac{r_{o}^{4} - r_{i}^{4}}{4} - \widetilde{A}_{m} \frac{r_{o}^{2+\gamma_{m}} - r_{i}^{2+\gamma_{m}}}{2 + \gamma_{m}} - \widetilde{B}_{m} \frac{r_{o}^{2-\gamma_{m}} - r_{i}^{2-\gamma_{m}}}{2 - \gamma_{m}} \right]$$
(5)

with

$$\gamma_m = \frac{(2m-1)\pi}{2\theta_0} \tag{6}$$

$$\widetilde{A}_{m} = \frac{r_{o}^{2+\gamma_{m}} - r_{i}^{2+\gamma_{m}}}{r_{o}^{2\gamma_{m}} - r_{i}^{2\gamma_{m}}}$$
(7)

$$\widetilde{B}_{m} = \frac{r_{o}^{\gamma_{m}} r_{i}^{2} - r_{i}^{\gamma_{m}} r_{o}^{2}}{r_{o}^{2\gamma_{m}} - r_{o}^{2\gamma_{m}}} (r_{i} r_{o})^{\gamma_{m}}$$
(8)

$$F_m = \frac{-4(-1)^m}{\theta_0 \gamma_m (\gamma_m^2 - 4)}$$
 (9)

where G, L_t , r_o , r_i , and θ_0 are the torsional rigidity, length of torsion member, outer radius, inner radius, and half the cross-sectional sweep angle, respectively. Additionally, r, w, and t are the centroidal radius, centroidal arc length, and thickness, respectively.

With the bending and torsional stiffnesses defined for the curved LET joint, the equivalent stiffness of both the outside and inside LET joints can be identified using Equations 2-3.

For the analyses done in this work, the geometric parameters, material properties, and deflection angle used are provided in Table I. The listed geometric parameters are related to an outside LET joint in Figure 5. Additionally, in order to prevent geometric and numerical irregularities (e.g. due to a cross section wrapping in on itself), the following constraints are imposed:

$$\theta_{0_{max}} = \pi \tag{10}$$

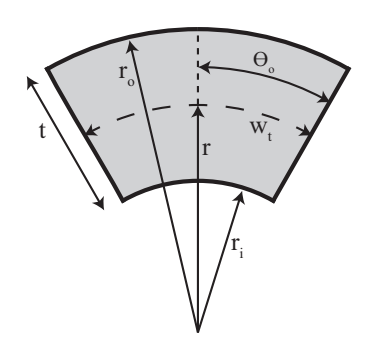


Fig. 4. The annular sector with parameters labeled. The torsion members of the curved LET have this cross section.

$$t_{max} = 2r \tag{11}$$

$$w_{max} = 2\pi r \tag{12}$$

$$w \ge t \tag{13}$$

Error in the predicted torsional stiffness may prevent accurate representations of the overall joint. To verify the accuracy of the predicted stiffness of only the torsional members, given by Equation 5, a comparison is made with finite element model results and is displayed in Figure 6. Using beam elements in ANSYS, an angular deflection load α was applied and the reaction moment was recorded as the thickness t was varied with respect to width w_t . This range of thickness represents the extremes of the cross sectional geometry, where the maximum value of t/w corresponds to a circular sector and the minimum to a thin annular sector. A maximum value for θ_0 allowed by the constraint equations 10-13 for the full range of thicknesses was used. The reaction moment in the numerical model was calculated using Equation 1 with the stiffness of the individual members being used rather than k_{eq} . The results show that for $0 < t/w_t < 1$, the error is less than 3%. Based on these results, Equation 5 is sufficiently accurate for this work.

Next, the full curved LET model is verified with a curved outside LET joint employing the geometry listed in Table I. The joint was curved about the longitudinal (hinge) axis, based on the centroidal axis

 $\begin{tabular}{l} TABLE\ I\\ Example\ curved\ LET\ Geometry\ Parameters. \end{tabular}$

Value
0.5 mm
10 mm
1 mm
1 mm
40 mm
1 mm
200 GPa
0.29
20^{o}

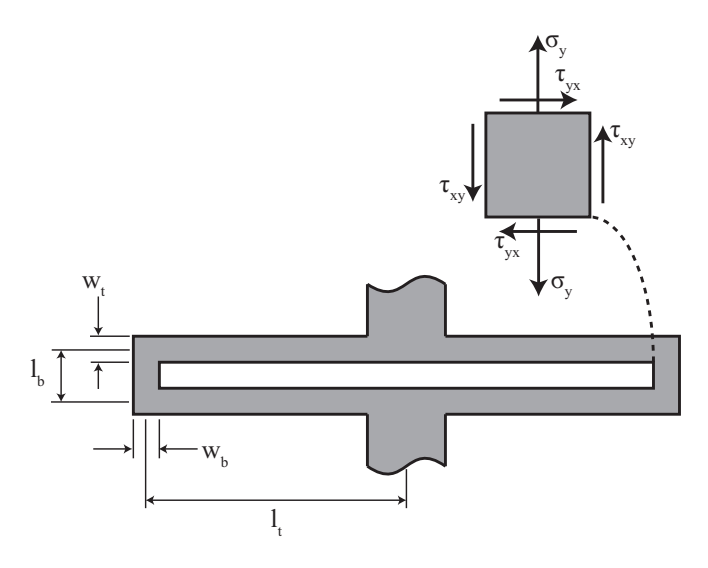


Fig. 5. Labels for geometric parameters of a LET joint. Note that l_b and w_t are measured as out-of-plane arc lengths. A stress element at the point of maximum stress in the joint is also shown.

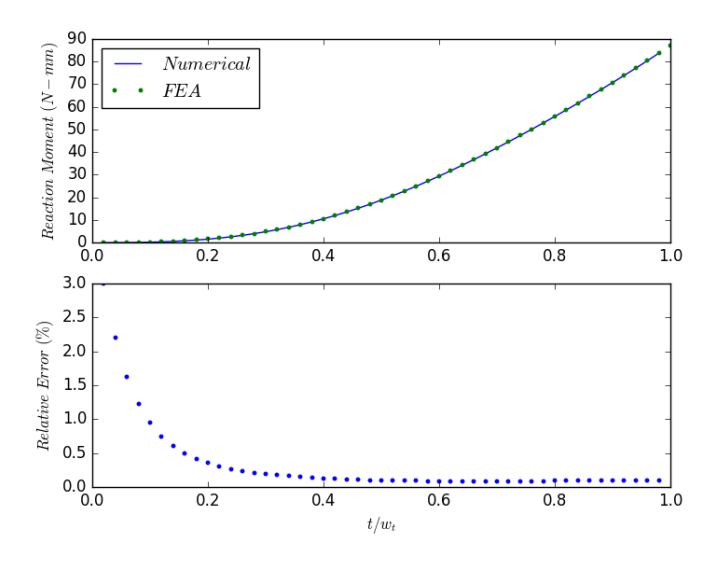


Fig. 6. A comparison of the numerical and finite element model results for the curved torsion members. An angular deflection load was applied and the reaction moment of the beam was recorded as the thickness t with respect to width w_t was varied. The results show little error using Equation 5.

of the substrate. Using solid elements in ANSYS, an angular deflection load α was applied and the reaction moment was recorded as the joint curvature K was varied in the range of 0 < K < 2.09, shown in Figure 7. This range of curvature simulates a joint curved from a planar state to a full cylinder with a longitudinal slit. The results show less than 2% relative error across the full range of joint curvature. Furthermore, the reaction moments of the finite element model are lower than those of the numerical model, meaning that the numerical model is conservative for calculating maximum stress,

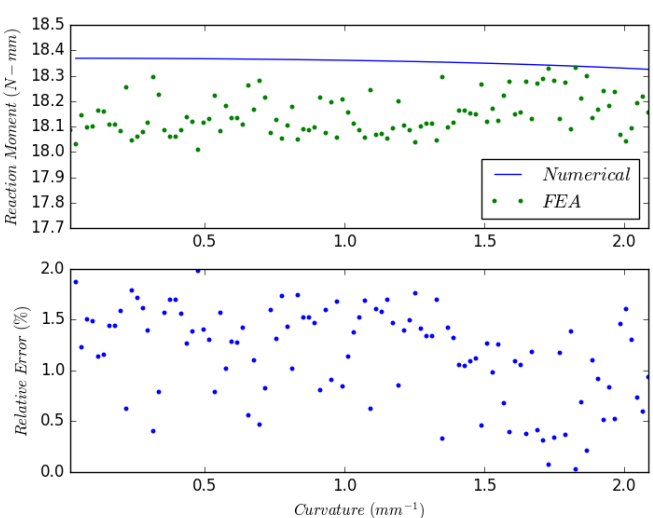


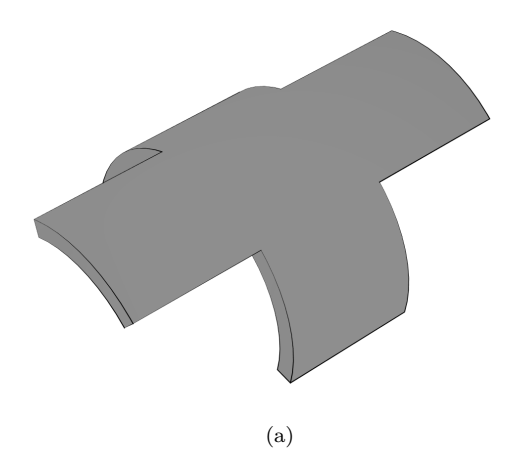
Fig. 7. A comparison of numerical and finite element model results for an outside LET joint, using Equation 2. An angular deflection load was applied and the reaction moment was recorded as the joint curvature was varied. The results show little error using Equation 2.

deflection, etc. Based on these results, Equations 2-5 are sufficiently accurate for predicting the equivalent stiffness of a curved LET joint, particularly in the design phase.

B. Shape Factors

Shape factors provide a method for quantifying effective material properties based on geometric alterations. For example, a beam with a rectangular cross section of a given length and modulus of elasticity will have a defined stiffness. If a designer seeks to maximize stiffness, the cross-sectional area could be rearranged into an I shape to create a beam with a greater stiffness. Since stiffness and modulus of elasticity have a linear relationship, the ratio of new stiffness to original stiffness creates a shape factor that can be multiplied by the material's modulus of elasticity to create an effective modulus of elasticity. This effective modulus is representative of a beam that has the same shape as the original (rectangular) beam, but exhibits the performance of the altered (I) beam. Through this method, many "new" materials can be developed that exhibit properties previously unattainable in other materials.

Elastic energy storage is constrained by the modulus of resilience of a given material. Resilience is a function of a material's yield strength S_y and modulus of elasticity E and is found by integrating the material's stress-strain curve from zero to the elastic limit. While the resilience of any material can be found through this integration, this work will demonstrate principles of the change in resilience through application in only simple linear elastic materials. Under this assumption, the resilience is then defined as



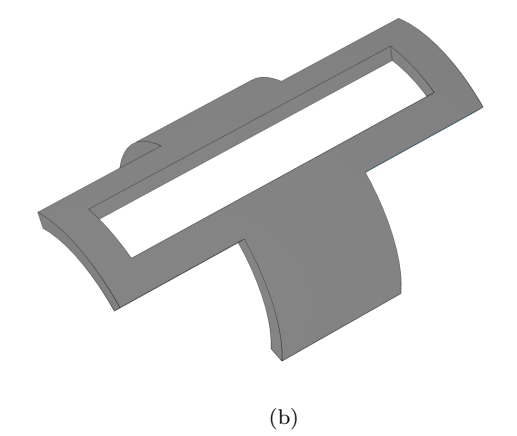


Fig. 8. (a) An uncut curved substrate with the same dimensions as (b) a curved LET joint.

$$U = \frac{S_y^2}{2E} \tag{14}$$

To create an effective resilience for a material, an effective modulus of elasticity and effective yield strength need to be identified.

The effective stiffness of the curved LET joint found in Section III-A can be compared to the stiffness of an uncut curved panel of the same thickness, curvature, width, and length, as shown in Figure 8. An elastic bending shape factor for the material can then be given as

$$\phi_S = \frac{k_{LET}}{k_{panel}} \tag{15}$$

where k_{LET} and k_{panel} are the stiffnesses of the curved LET and uncut panel, respectively.

Equation 15 can now be used to calculate the effective elastic modulus of the curved material due to the LET joint as

$$E_{eff} = \phi_S E \tag{16}$$

The effective yield strength of the curved material is found through a separate shape factor comparing the bending moments at failure for the joint and the substrate shown in Figure 8. The magnitude of the bending moment at failure for a linear elastic curved material is limited by the geometry of the beam and is given for the outer and inner surfaces as [33]

$$||M||_{panel,o,max} = \frac{S_y r_o A \left(r_i + \frac{t}{2} - \frac{t}{\ln\left(\frac{r_o}{r_i}\right)}\right)}{r_o - \frac{t}{\ln\left(\frac{r_o}{r_i}\right)}}$$

$$||M||_{panel,i,max} = \frac{S_y r_i A \left(r_i + \frac{t}{2} - \frac{t}{\ln\left(\frac{r_o}{r_i}\right)}\right)}{r_i - \frac{t}{\ln\left(\frac{r_o}{r_o}\right)}}$$

$$(17)$$

where S_y is the yield strength and A is the cross-sectional area. The lesser of these two moments is the constraining value and should be used to evaluate the maximum bending moment of the substrate.

Once a LET joint is fabricated from the substrate, the maximum stress results at the corners where the torsional and bending members meet. Figure 5 shows a stress element at a corner of the joint which is in a state of plane stress. Using the distortion energy theory, the von Mises stress at that point is [33]

$$\sigma' = (\sigma_x^2 - \sigma_x \sigma_y + \sigma_y^2 + 3\tau_{xy}^2)^{\frac{1}{2}}$$
 (18)

which simplifies to

$$\sigma' = (\sigma^2 + 3\tau^2)^{\frac{1}{2}} \tag{19}$$

where σ and τ are the stresses in each of the bending and torsional members, respectively. Because the bending members are in parallel, they each carry half of the moment applied to the joint. The stress in a single bending member can then be modeled by

$$\sigma = \frac{Mt}{4I_b} \tag{20}$$

With torsional members also in parallel, the stress in a single torsional member is given numerically as [32]

$$\tau = \frac{M}{2} \frac{1}{k_{LET}} G \sum_{m=1}^{\infty} F_m \cos(\gamma_m \theta) \left[2R - \widetilde{A}_m \gamma_m R^{\gamma_m - 1} + \widetilde{B}_m \gamma_m R^{-\gamma_m - 1} \right]$$
(21)

where θ and R specify a point on the cross-section for which the stress is to be calculated. Because the maximum moment of the members is to be calculated, the point where the maximum stress occurs is of interest. θ and r are then set to values of 0 and r_o , respectively, which correspond to the center of the outermost surface. Setting $\sigma' = S_y$, substituting Equations 20-21 into Equation 19, and solving for M, the maximum moment before yield in the curved LET joint becomes

$$M_{LET,max} = \frac{S_y}{\left[\frac{9}{w_b t^4} - \frac{3G^2}{4k_{LET}} \left(\sum_{m=1}^{\infty} F_m \left[2r_o - \widetilde{A}_m \gamma_m r_o^{\gamma_m - 1} + \widetilde{B}_m \gamma_m r_o^{-\gamma_m - 1}\right]\right)^2\right]^{\frac{1}{2}}}$$
(22)

Equations 17 and 22 can then be used to derive the strength efficiency shape factor for a linear elastic material as

$$\phi_B = \frac{M_{LET,max}}{M_{panel,max}} \tag{23}$$

An effective yield strength is then given by multiplying the strength efficiency shape factor with the yield strength of the uncut curved substrate:

$$\sigma_{eff} = \phi_B S_y \tag{24}$$

The effective modulus of resilience of a linear-elastic curved member altered by a LET joint can now be calculated by substituting the effective modulus from Equation 16 and effective yield strength from Equation 24 into Equation 14 as

$$U_{eff} = \frac{\left(\phi_B S_y\right)^2}{2\phi_S E} \tag{25}$$

Equation 25 can now be applied to various linearelastic materials to demonstrate their energy storage and stiffness behaviors after application of the curved LET joint.

C. Performance Index

Material selection becomes more complex when a design must meet multiple criteria. Performance indices can provide a systematic material selection process that weights multiple objectives, resulting in quantified and comparable performance values. For example, a designer seeking to create a light, stiff beam would create a material index relating the modulus of elasticity E with the density of the material ρ to create a material index E/ρ [9]. Maximizing this value would allow a designer to select a material that best meets stiffness and weight requirements for a given application.

The curved LET joint presented in this work is intended to provide high strain energy before failure while maintaining low stiffness for actuation. These competing constraints create a multi-objective problem that may be addressed with an appropriate performance index. High energy storage before yield, represented by the modulus of resilience, can be compared with the flexibility of the

material, represented by the modulus of elasticity, to create a performance index given as

$$P = \frac{U}{E} = \left(\frac{S_y}{E}\right)^2 \tag{26}$$

This material index provides the slope of lines that can be drawn on a U vs. E Ashby plot to demonstrate material performance relative to the competing objectives of energy storage before yield and low stiffness. Materials that lie along the same material index line provide the same performance with respect to the desired objectives. By convention, maximizing the material index results in improved performance.

IV. RESULTS AND DISCUSSION

Figure 9 is a logarithmic Ashby plot which demonstrates the changes in the modulus of resilience and modulus of elasticity for various sample materials subject to these material and geometric parameters. Grayscale regions in the plot represent standard material properties and the colored regions represent effective material properties after application of ϕ_S and ϕ_B . Since manufacturing limitations constrain these shape factors, the effective properties in this case have been calculated based on water-jet machining tolerances for polymers and metals (≥ 1 mm). The envelopes for the remaining materials were extrapolated accordingly. LET joint geometry and manufacturing precision for each material should be considered before using the chart.

Here the effective modulus of elasticity of the materials decreases by approximately three orders of magnitude. Since stiffness is directly proportional to the modulus of elasticity, the LET joint may significantly reduce the stiffness of a curved member and allow for compliant motion. The effective modulus of resilience of the material has decreased by approximately one order of magnitude.

The material performance index P is plotted on Figure 9 to demonstrate how materials can provide more efficient energy storage in the curved member by applying a LET joint. Materials improve in performance as they move toward the top left corner of the plot. While each material has been adjusted by the same amount with reference to its original value, it can be seen that the curved LET joint enables each material to improve its performance relative to the performance index.

With these results, designers can select suitable materials for applications that would otherwise not have sufficient energy storage and stiffness characteristics while considering other design constraints. For example, a bistable mechanism designed for aerospace applications could require compliant joints fabricated in a metal material to prevent outgassing and to minimize mass. If the designer desires to use the strain energy in a joint to enable bistable behavior, the methods developed in this work could be employed to create shape factors reflective of their design. The changed properties could then be

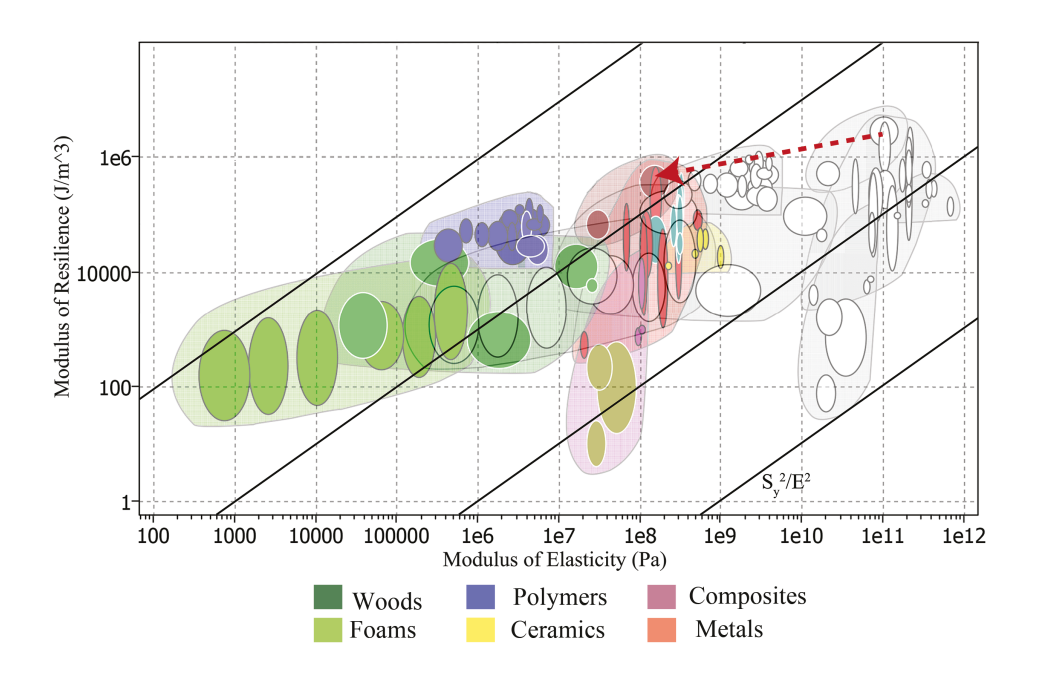


Fig. 9. An Ashby plot of modulus of resilience vs. modulus of elasticity. Grayscale sections represent original material properties. Colored regions represent new (effective) material properties due to the curved LET joint. There is a marked decrease in the modulus of elasticity and a smaller decrease in the modulus of resilience.

plotted on an Ashby chart similar to Figure 9 to indicate whether their curved LET design will safely meet resilience constraints while still providing the desired flexibility of the joint. The red dotted line on Figure 9 demonstrates a possible change in material properties for this example, assuming the geometry used in this work.

V. CONCLUSION

This research has demonstrated a method of increasing the efficiency of energy storage in cylindrically-curved sheet materials through the implementation of lamina emergent torsional joints. Shape factors provided a means of quantifying the effects of geometric changes in a substrate, in this case, removing material to make a cylindrically curved LET joint. The joint was treated as a "new" material with effective material properties and improved energy storage efficiency relative to the substrate.

A numerical model has been presented and verified for determining curved LET joint stiffness and maximum moment. Formulas for predicting the stiffness and maximum moment of an un-cut curved reference material have also been provided. With these, functions for shape factors for the modulus of elasticity and the modulus of resilience were developed. These provide a means by which designers can rapidly select materials for design applications using performance indices.

Using this method, specific shape factors based on given geometry were developed, and the resulting effective modulus of resilience and modulus of elasticity for various materials were represented on an Ashby plot. The resilience decreased by about an order of magnitude, while the stiffness decreased by approximately three orders of magnitude. These results indicate that a designer requiring decreased stiffness while retaining much of the energy storage capability can achieve it using curved LET joints. They also show that designers can tailor stiffness and energy storage properties to alternative materials that were previously not suitable for a given application.

Various applications could benefit from the results of this work. Aeropace, surgical tools, defense, and consumer products are just a few areas that may demand monolithic, compactly stowed compliant joints. Curved LET joints could be uniquely suited to satisfying those demands.

ACKNOWLEDGMENT

This paper is based on work supported by the U.S. National Science Foundation and the U.S. Air Force Office of Scientific Research through NSF Grant No. EFRI-ODISSEI-1240417 and NSF Grant No. 1663345.

References

[1] S. Henein, L. Rubbert, F. Cosandier, and M. Richard, The Art of Flexure Mechanism Design. CRC Press, 2017.

- [2] R. Fowler, L. Howell, and S. Magleby, "Compliant space mechanisms: a new frontier for compliant mechanisms," Mech. Sci, vol. 2, no. 2, pp. 205–215, 2011.
- [3] S. Awtar, T. T. Trutna, J. M. Nielsen, R. Abani, and J. Geiger, "FlexdexTM: a minimally invasive surgical tool with enhanced dexterity and intuitive control," Journal of Medical Devices, vol. 4, no. 3, p. 035003, 2010.
- [4] B. D. Jensen, L. L. Howell, and L. G. Salmon, "Introduction of two-link, in-plane, bistable compliant mems," in Proceeding of the 1998 ASME Design Engineering Technical Conferences, DETC98/MECH-5837, 1998.
- [5] L. L. Howell, Compliant mechanisms. John Wiley & Sons, 2001
- [6] M. Cestari, D. Sanz-Merodio, J. C. Arevalo, and E. Garcia, "An adjustable compliant joint for lower-limb exoskeletons," IEEE/ASME Transactions on Mechatronics, vol. 20, no. 2, pp. 889–898, 2015.
- [7] G. Chen, S. Zhang, and G. Li, "Multistable behaviors of compliant sarrus mechanisms," Journal of Mechanisms and Robotics, vol. 5, no. 2, p. 021005, 2013.
- [8] J. O. Jacobsen, G. Chen, L. L. Howell, and S. P. Magleby, "Lamina emergent torsional (LET) joint," Mechanism and Machine Theory, vol. 44, no. 11, pp. 2098–2109, 2009.
- [9] M. F. Ashby, Materials Selection in Mechanical Design, 4th Edition. Elsevier, 2011.
- [10] D. F. Machekposhti, N. Tolou, and J. Herder, "Monolithic and statically balanced rotational power transmission coupling for parallel axes," in Microactuators and Micromechanisms. Springer, 2017, pp. 189–198.
- [11] M. T. Pham, T. J. Teo, S. H. Yeo, P. Wang, and M. L. S. Nai, "A 3-D printed Ti-6Al-4V 3-DOF compliant parallel mechanism for high precision manipulation," IEEE/ASME Transactions on Mechatronics, vol. 22, no. 5, pp. 2359–2368, 2017.
- [12] K. Y. Choi, A. Akhtar, and T. Bretl, "A compliant four-bar linkage mechanism that makes the fingers of a prosthetic hand more impact resistant," in Robotics and Automation (ICRA), 2017 IEEE International Conference on. IEEE, 2017, pp. 6694–6699.
- [13] H. M. Anver, R. Mutlu, and G. Alici, "3D printing of a thin-wall soft and monolithic gripper using fused filament fabrication," in Advanced Intelligent Mechatronics (AIM), 2017 IEEE International Conference on. IEEE, 2017, pp. 442–447.
- [14] J. Butler, S. Magleby, L. Howell, S. Mancini, and A. Parness, "Highly compressible origami bellows for microgravity drillingdebris containment," in AIAA SPACE and Astronautics Forum and Exposition, 2017, p. 5341.
- [15] T. Bacek, M. Moltedo, J. Gonzalez-Vargas, G. A. Prieto, M. Sanchez-Villamañan, J. Moreno, and D. Lefeber, "The new generation of compliant actuators for use in controllable bioinspired wearable robots," in Wearable Robotics: Challenges and Trends. Springer, 2017, pp. 255–259.
- [16] G. Chen, B. Xiong, and X. Huang, "Finding the optimal characteristic parameters for 3r pseudo-rigid-body model using an improved particle swarm optimizer," Precision Engineering, vol. 35, no. 3, pp. 505–511, 2011.
- [17] H.-J. Su, "A pseudorigid-body 3r model for determining large deflection of cantilever beams subject to tip loads," Journal of Mechanisms and Robotics, vol. 1, no. 2, p. 021008, 2009.
- [18] Y.-Q. Yu, Z.-L. Feng, and Q.-P. Xu, "A pseudo-rigid-body 2r model of flexural beam in compliant mechanisms," Mechanism and Machine Theory, vol. 55, pp. 18–33, 2012.
- [19] S. Canfield and M. Frecker, "Topology optimization of compliant mechanical amplifiers for piezoelectric actuators," Structural and Multidisciplinary Optimization, vol. 20, no. 4, pp. 269–279, 2000.
- [20] C. B. Pedersen, T. Buhl, and O. Sigmund, "Topology synthesis of large-displacement compliant mechanisms," International Journal for numerical methods in engineering, vol. 50, no. 12, pp. 2683–2705, 2001.
- [21] J. B. Hopkins and M. L. Culpepper, "Synthesis of multidegree of freedom, parallel flexure system concepts via freedom and constraint topology (fact)-part i: Principles," Precision Engineering, vol. 34, no. 2, pp. 259–270, 2010.

- [22] M. Frecker, G. Ananthasuresh, S. Nishiwaki, N. Kikuchi, and S. Kota, "Topological synthesis of compliant mechanisms using multi-criteria optimization," Journal of Mechanical design, vol. 119, no. 2, pp. 238–245, 1997.
- [23] O. Sigmund, "On the design of compliant mechanisms using topology optimization," Journal of Structural Mechanics, vol. 25, no. 4, pp. 493–524, 1997.
- [24] J. O. Jacobsen, B. G. Winder, L. L. Howell, and S. P. Magleby, "Lamina emergent mechanisms and their basic elements," Journal of Mechanisms and Robotics, vol. 2, no. 1, pp. 011 003– 1 to 011 003–9, 2010.
- [25] Q. T. Aten, B. D. Jensen, S. Tamowski, A. M. Wilson, L. L. Howell, and S. H. Burnett, "Nanoinjection: pronuclear DNA delivery using a charged lance," Transgenic research, vol. 21, no. 6, pp. 1279–1290, 2012.
- [26] N. B. Albrechtsen, S. P. Magleby, and L. L. Howell, "Identifying potential applications for lamina emergent mechanisms using technology push product development," in ASME 2010 International Design Engineering Technical Conferences and Computers and Information in Engineering Conference. American Society of Mechanical Engineers, 2010, pp. 513–521.
- [27] I. L. Delimont, S. P. Magleby, and L. L. Howell, "Evaluating compliant hinge geometries for origami-inspired mechanisms," Journal of Mechanisms and Robotics, vol. 7, no. 1, p. 011009, 2015.
- [28] Z. Xie, L. Qiu, and D. Yang, "Design and analysis of outsidedeployed lamina emergent joint (od-lej)," Mechanism and Machine Theory, vol. 114, pp. 111–124, 2017.
- [29] L. Qiu, G. Huang, and S. Yin, "Design and performance analysis of double c-type flexure hinges," Journal of Mechanisms and Robotics, vol. 9, no. 4, p. 044503, 2017.
 [30] Z. Xie, L. Qiu, and D. Yang, "Design and analysis of a variable
- [30] Z. Xie, L. Qiu, and D. Yang, "Design and analysis of a variable stiffness inside-deployed lamina emergent joint," Mechanism and Machine Theory, vol. 120, pp. 166–177, 2018.
- [31] T. G. Nelson, R. J. Lang, N. A. Pehrson, S. P. Magleby, and L. L. Howell, "Facilitating deployable mechanisms and structures via developable lamina emergent arrays," Journal of Mechanisms and Robotics, vol. 8, no. 3, p. 031006, 2016.
- [32] C. S. Jog, Continuum mechanics. Cambridge University Press, 2015, vol. 1.
- [33] J. E. Shigley, Shigley's mechanical engineering design. Tata McGraw-Hill Education, 2011.